DESIGN, DEVELOPMENT AND TESTING OF THE GMI REFLECTOR DEPLOYMENT ASSEMBLY

Larry Guy[(1)], Mike Foster[(2)], Mike McEachen[(2)], Joseph Pellicciotti[(3)], Michael Kubitschek[(4)],

[(1)]Ball Aerospace, 1600 Commerce St. Boulder CO 80301, Email:lguy@ball.com
[(2)]ATK Aerospace Systems Group, Goleta California
[(3)]NASA NESC- Goddard Space Flight Center, Greenbelt, Maryland
[(4)]Ball Aerospace, 1600 Commerce St. Boulder CO 80301, Email: mkubitsc@ball.com

ABSTRACT

The GMI Reflector Deployment Assembly (RDA) is an articulating structure that accurately positions and supports the main reflector of the Global Microwave Imager (GMI) throughout the 3 year mission life. The GMI instrument will fly on the core Global Precipitation Measurement (GPM) spacecraft and will be used to make calibrated radiometric measurements at multiple microwave frequencies and polarizations. The GPM mission is an international effort managed by the National Aeronautics and Space Administration (NASA) to improve climate, weather, and hydro-meteorological predictions through more accurate and frequent precipitation measurements1. Ball Aerospace and Technologies Corporation (BATC) was selected by NASA Goddard to design, build, and test the GMI instrument. The RDA was designed and manufactured by ATK Aerospace Systems Group to meet a number of challenging packaging and performance requirements. ATK developed a flight-like engineering development unit (EDU) and two flight mechanisms that have been delivered to BATC. This paper will focus on driving GMI instrument system requirements, the RDA design, development, and test activities performed to demonstrate that requirements have been met.

1. GMI INSTRUMENT ARCHITECTURE

The GMI instrument is one of the payload instruments on the GPM core spacecraft and will be launched on a Japanese H-IIA launch vehicle. The instrument is a continuously rotating sensor that mounts to the anti-nadir side of the spacecraft and utilizes a 1.2 meter diameter parabolic reflector to focus energy from the earth onto an array of feed horns attached to the rotating structure. To fit within the launch vehicle fairing, the main reflector must be stowed toward the front of the spacecraft bus as shown in Figure 1. Launch restraints secure the main reflector and RDA to the GMI main structure. After launch, the restraints deploy and the RDA must maneuver the reflector from its stowed location and position it into a precise orientation above the instrument for operation. The on-orbit deployed reflector must match the ground alignment orientation to within .020" in position and 40 arc-seconds in order to maintain tight off nadir angle pointing requirements. The RDA must maintain stable reflector orientation throughout the 3 year GMI life.

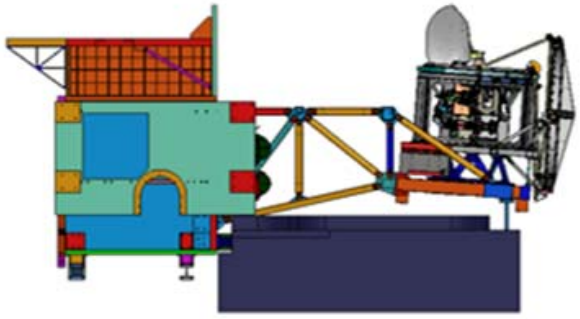

Figure 1: GPM Spacecraft with Stowed GMI

Figure 2 shows the GMI instrument in the deployed configuration. The support struts of the RDA must clear the stationary calibration elements as well as the fields of view of the main and cold sky reflectors.

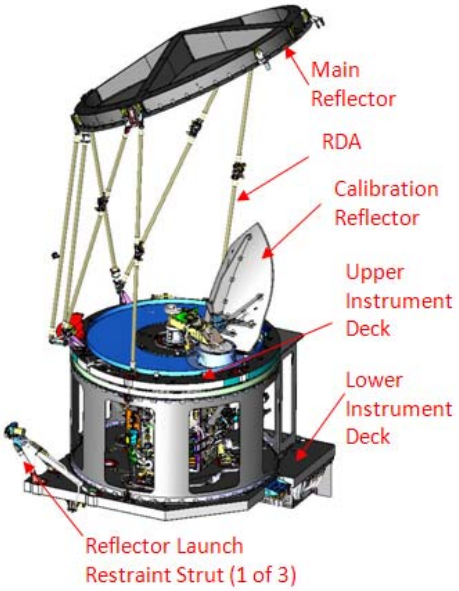

Figure 2: Deployed Configuration of GMI

2. RDA Description

The GMI RDA is a kinematically determinate structure consisting of an aft bipod structure and forward and aft side strut assemblies that attach to four locations on the instrument upper deck and three locations on the outer perimeter of the main reflector. The RDA is constructed from composite tubes bonded to titanium fittings that are attached to a variety of joints designed to allow the structure to fold into a stowed configuration. When stowed, the reflector is in a defined location where it is restrained for launch, and the RDA strut tubes are positioned into limited available areas within the stowed envelope. Deployment force is provided by a torsion spring attached to the aft bipod assembly with speed controlled by a fluid damper. Deployment reliability is enhanced by eliminating the possibility of binding of the strut joints. This is accomplished by using combination of spherical and revolute hinges configured such that the structure is effectively under constrained. To provide control during deployment, a novel auxiliary synchronization linkage directs the motion of the reflector during the majority of the operation until the spring loaded side strut elbow joints lock out completing the deployment and forming a geometrically determinate structure. Figure 3 shows the primary elements of the assembly.

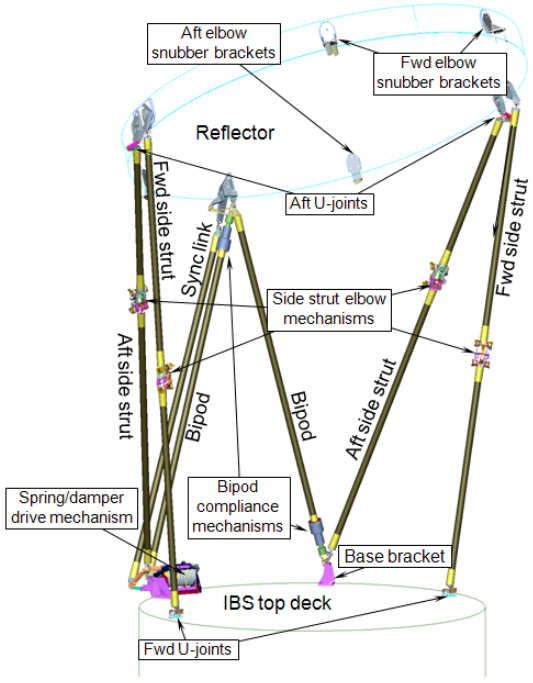

Figure 3: RDA Components

2.1 RDA Design Drivers

The location of the stowed reflector is defined by available volume on the spacecraft and launch vehicle thus driving the geometry of the stowed RDA. The RDA must reliably deploy the 12 kg reflector from this location to a repeatable position, and maintain its orientation when exposed to the on-orbit environment throughout the mission life. Table 1 lists the primary performance requirements of the RDA.

Table 1: Key RDA Performance Requirements

Mass	5.7 kg max
Deployed Stiffness	11 Hz min
Deployment Repeatability	<.020 in, <40 arc sec
Deployment Stability	<.010 in, <20 arc sec
Deployment Duration	<5 min

2.2 Kinematic Analysis

To support the design phase, a rigorous dynamic analysis of the RDA structure was performed using the ADAMS kinematic modeling tool. This analysis aided in finalizing strut geometry, joint configurations, and predicting requirement performance such as torque margin and interface loads. The model included detailed representations of mounting interfaces, joint type, preload, spring forces, strut stiffness, clearances and reflector structural properties with special attention given to static and dynamic friction.

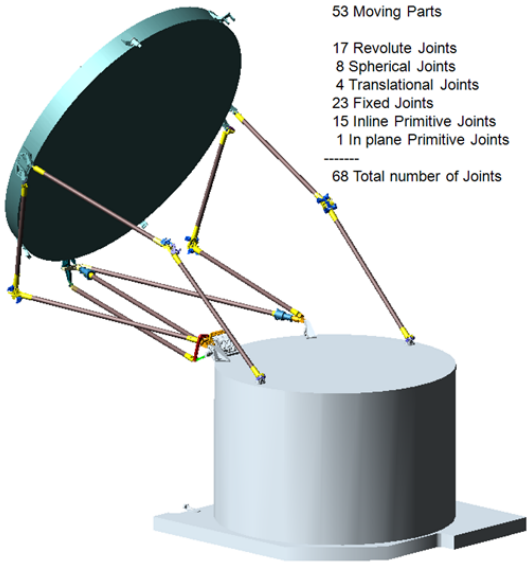

Figure 4: ADAMS Kinematic Model

A variety of joint configurations were evaluated using the kinematic model in order to seek a configuration that maximizes deployment reliability. In this case, a highly reliable mechanism design is one that is not susceptible to binding and is insensitive to varying joint friction and interface geometry changes. Satisfying these criteria led to a solution that consists of a combination of revolute (1 DOF), universal (2 DOF) and spherical (3 DOF) hinge joints in very specific locations (see Figure 5). The analysis showed that this particular configuration was under constrained about all 3 axes during deployment and hence immune

to binding. When fully deployed however, the result is a statically determinate structure where the final position of the reflector is based on the RDA geometry mounted at the deck and reflector interfaces. The analysis predicted that even large variations of these interface points did not impede deployment, only the final deployed orientation.

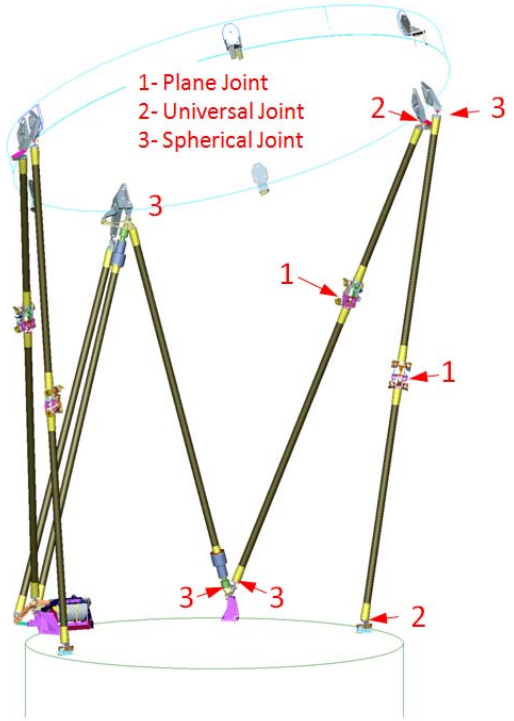

Figure 5: Joint Configuration

To maintain the inherent anti-binding characteristic of the design but constrain the path of the deploying reflector, a "synchronization linkage" and an "out-rigger bearing" were added as shown in Figure 6.

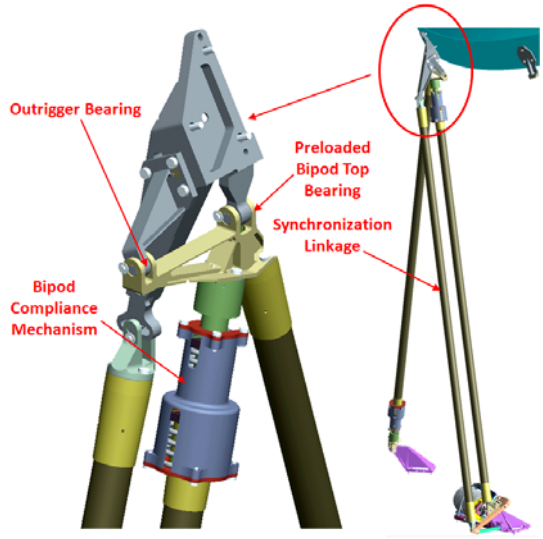

Figure 6: Sync Link & Outrigger Bearing

Once deployed, clearances ensure that they are de-coupled to not influence the final position of the reflector. Rigorous exercising of the kinematic model showed the deployment robustness of the mechanism design when exposed to varying friction, varying spring forces, geometry changes and spacecraft acceleration.

2.3 Design Details

2.3.1 Concept of Operation

When stowed, the mounting interfaces of the RDA are constrained by the instrument upper deck and the launch locked main reflector. This provides support of the aft bipod and side strut end fittings. Snubbers attached to the reflector and instrument deck restrain the motion of the side struts thus fully supporting the RDA during launch (see Figure 7).

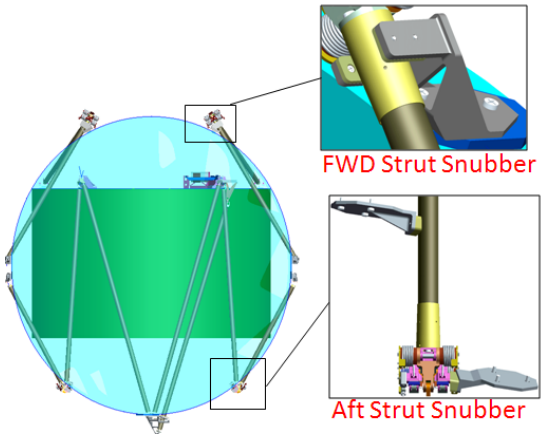

Figure 7: Side Strut Snubbers

Launch vibration loads result in as much as +/- 5 mm of predicted relative displacement between the upper and lower instrument decks. Since the ends of the RDA bipod are attached to these two structures, it must accommodate the relative motion. To accomplish this, compliant mechanisms are incorporated in the bipod design. The bipod compliance mechanisms are spring pre-loaded bi-axial devices designed to accommodate the relative motion while maintaining high axial stiffness and position repeatability when deployed. These mechanisms behave as rigid structural elements in all deployed operational environments. During launch when axial forces exceed a threshold in either tensile or compressive directions the mechanisms deflect axially in a controlled manner. Figure 8 shows the mechanism.

Figure 8: Bipod Compliance Mechanism

Once on orbit, the instrument will remain stowed until it becomes thermally stable. During this period, heaters installed onto the RDA maintain the temperature of the viscous damper within its operating temperature. When ready, the reflector launch restraints will be released and the RDA spring/damper assembly will initiate deployment. Deployment force is generated using redundant titanium torsion springs attached to the lower bipod mount. A viscous damper located in the inner diameter of the spring coil assembly controls the deployment rate (see Figure 9). The springs are sized to provide positive torque margin even in the event that one spring fails.

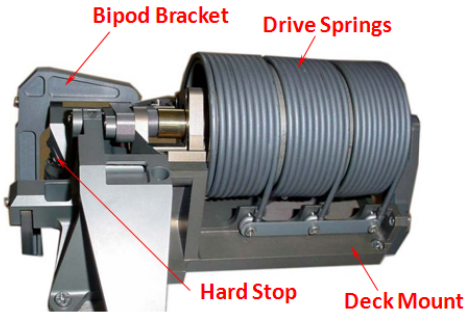

Figure 9: Spring / Damper Assembly

As the bipod is being deployed, the synchronization linkage is acting to guide the motion of the reflector and deploying side struts. This link, in conjunction with the outrigger bearing controls the path of the reflector throughout the deployment range. Figure 10 shows details of the lower section of the linkage mechanism. It is important that the spring drive and synchronization mechanisms are decoupled from the deployed RDA so they do not affect the statically determinate position of the reflector.

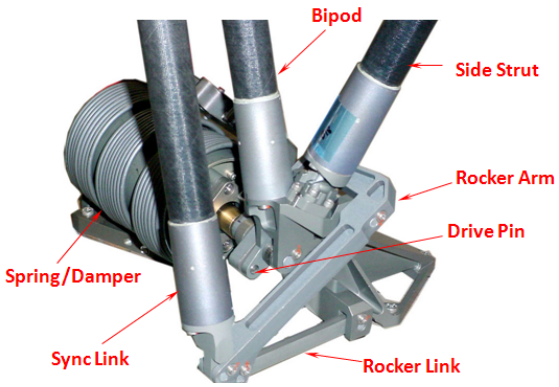

Figure 10: Synchronization Linkage Lower Section

Motivation for the final deployment stage is provided by the side strut elbow joints. These multi featured revolute hinge joints include a hard stop for precise positioning, a latch to ensure the joint remains in the deployed configuration, redundant torsion springs and a sophisticated linkage system. The linkage is designed to minimize the spring applied opening torque of the hinge during most of the deployment and maximize it at the end to complete the deployment and provide preload on the hinge joint. Figure 11 shows elements of the hinge and linkage operation details.

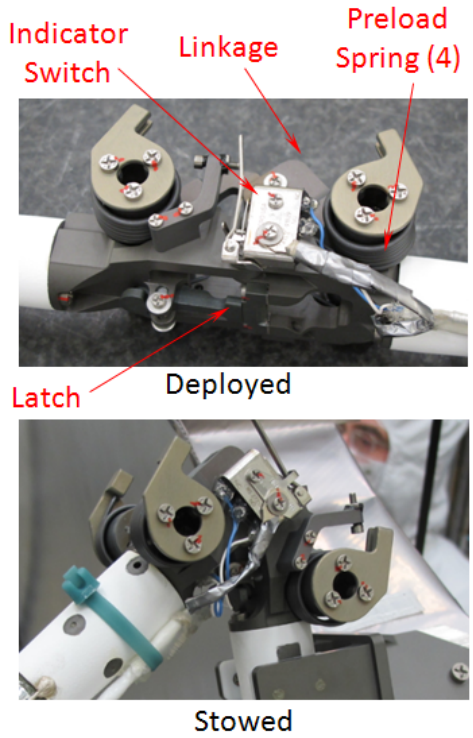

Figure 11: Forward Strut Elbow Joint

Deployment is complete when the four side strut elbows lock in place. At this point, the drive mechanism, synchronization linkage and outrigger bearing are decoupled from the load path and the structure fully geometrically defined.

2.3.2 Preload Mechanisms

Each rotating joint is preloaded to provide deployed stiffness and to optimize repeatability. The elbow joints are preloaded via torsional springs and a hard stop as described above. The 3 DOF joints employ custom spherical bearings attached to the end of the strut tubes. The spherical bearings are assembled into housings designed to allow the required motion of the applicable strut tube while maximizing contact area with the ball. The preload mechanism is designed to maximize deployed stiffness while minimizing deployment friction.

Each lower bipod hinge supports both a bipod strut and an aft side strut. Because of this, operational loads applied to the hinge by the struts are in two directions and the force magnitudes vary depending on whether operation is performed on the ground versus on orbit and whether the instrument is spinning or not (see Figure 12). To eliminate the potential shift that could occur with a standard revolute joint when subjected to varying load cases, these hinges utilize a joint with

special geometry that provides stable positioning of the struts over a wide range of load cases.

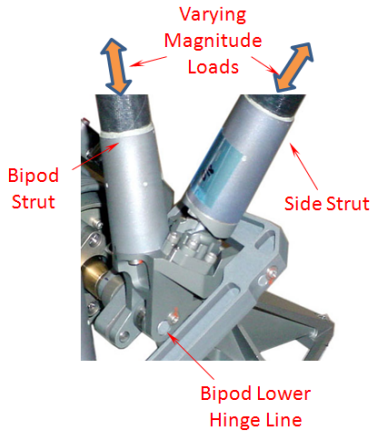

Figure 12: Lower Bipod Hinge Load Condition

2.4 Manufacturing

The RDA strut tubes are cylindrical graphite epoxy tubers with a titanium fitting bonded to each end. They were manufactured with the aid of precisely aligned bond tooling. Once bonded and cured, they were thermal cycled, proof tested and then assembly began by bolting the appropriate hinge fitting to each end of the strut tube.

Individual strut tubes were then joined into a strut assembly and installed into another precision fixture for final alignment and length tuning operations.

The completed strut assemblies were then vibration tested as a group to proto-qualification levels and assembled into a complete RDA structure. To support final alignment and performance test activities, ATK manufactured instrument deck and reflector simulators. These simulators, shown in Figure 13, were carefully designed with RDA mounting interfaces that matched the flight requirements. The reflector simulator also mimicked the mass properties and stiffness of the flight reflector. Reflector launch locks were simulated using simple pins that were manually operated.

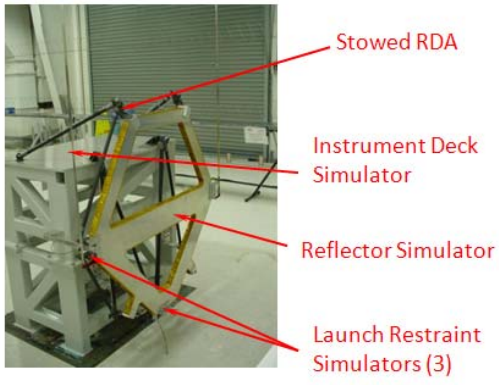

Figure 13: Reflector & Instrument Simulators

Gravity offloading ground support equipment (GSE) was manufactured to support deployment and torque margin testing. This GSE consisted of overhead supports attached to the reflector simulator near the RDA mounts. This off-loader assembly was designed to minimize the influence of gravity on the RDA, without introducing loads that would affect the deployment kinematics. See Figures 14 & 15.

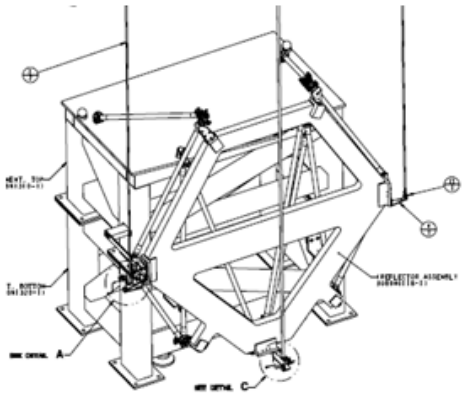

Figure 14: Gravity Offloader Support Points

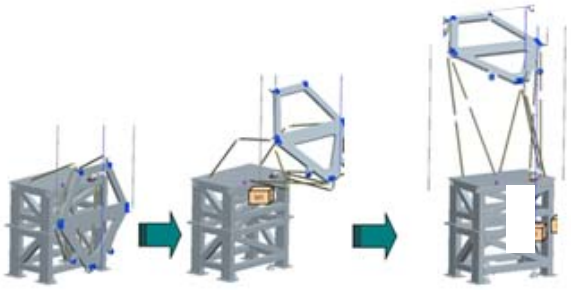

Figure 15: Deployment Sequence

3. RDA Performance Testing

The primary performance tests imposed on the RDA included deployment repeatability, deployment duration, deployed stiffness, torque margin, deployment over operating temperature, off-nominal deployment and kinematic model validation.

3.1 Deployment Testing

Deployed reflector measurements were accomplished using a laser tracker to determine the location of points on the reflector near the RDA mounting interfaces relative to features on the deck simulator. Deployment repeatability was assessed by comparing the laser tracker results of multiple deployments. A log book was used to record and trend the duration of each deployment. Typical measurement setup is shown in Figure 16.

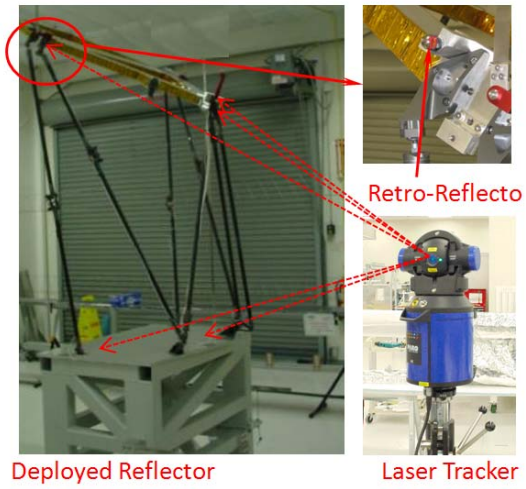

Figure 16: Deployment measurement Setup

Test results of the EDU, Flight 1 and Flight 2 assemblies showed that RDA repeatably positioned the reflector to within .001 inches and 8 arc seconds compared to an allocated requirement of < .003 inch and < 10 arc second. Results of Flight 1 repeatability testing (10 deployments) is shown in Figure 17.

Displacements			Rotations		
dx	dy	dz	rx	ry	rz
in	in	in	arc-sec	arc-sec	arc-sec
0.0001	-0.0006	0.0000	-1.75	2.64	3.92
0.0001	-0.0002	0.0000	-0.31	-1.07	1.24
0.0000	0.0001	0.0000	0.31	-0.25	-1.24
0.0004	0.0008	0.0001	0.52	0.37	-7.01
0.0001	0.0000	0.0001	0.31	0.17	0.21
-0.0001	0.0001	-0.0001	0.10	-0.87	0.62
0.0002	0.0003	-0.0001	-0.10	-1.07	-2.48
-0.0003	-0.0003	-0.0001	0.31	-0.04	1.86
-0.0001	0.0002	0.0001	0.72	-0.87	0.62
-0.0005	-0.0003	0.0004	-0.10	0.99	2.27

Figure 17: Flight Unit 1 Repeatability Results

Tests were also conducted in a thermal chamber at the ATK predicted operating temperature extremes of +71C and -73C. During cold temperature testing, heaters attached to the spring/damper mechanism damper maintained the damper temperature above 0C. These tests successfully demonstrated that the assembly properly deployed at these worst case temperature extremes.

3.2 Torque Margin Testing

Verifying 2X torque margin of the drive assembly proved to be a challenging test. The initial plan was to remove half of the deployment springs and, with the aid of the gravity offloader, demonstrate that the assembly would still deploy. However, kinematic modeling and EDU testing showed that neutral buoyancy of the reflector was not achievable throughout the deployment range with a single setting of the offloader. The analysis did show though that neutral buoyancy could be achieved for a limited range of the deployment. So as a compromise, the offloader was calibrated over 5 angular deployment ranges. Then, with half of the deployment springs removed, the reflector was manually positioned at the start of a range, the offloader adjusted and then the reflector released to demonstrate deployment over that range of motion. The reflector was then manually stopped at the beginning of the next range and the process repeated. This test successfully demonstrated that the 2X torque margin requirement was met.

3.3 Deployed Stiffness Testing

Deployed stiffness testing to demonstrate compliance to the 11 Hz minimum requirement was performed using two different methods. The first was an indirect test where a lateral load was applied at the reflector simulator interface and the corresponding deflection measured using a laser tracker. The data was then compared to structural analysis stiffness for the predicted deployed mode. A schematic of this test setup is shown in Figure 18.

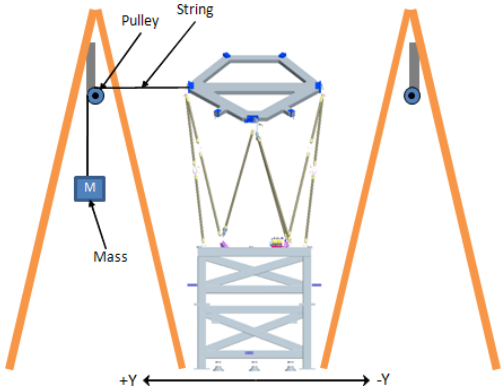

Figure 18: Stiffness Test Setup

The second stiffness test approach involved a more direct measurement where the laser tracker simply recorded the oscillation response of the reflector after being subjected to an impulse load. FFT evaluation of the laser tracker data clearly showed the resonant frequency of the system. Figure 19 shows a representative FFT plot. This direct measurement is simple to implement and correlates well with analytical predictions. It was used exclusively for comparing pre and post environmental test stiffness measurements.

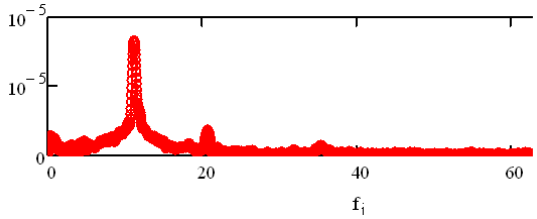

Figure 19: Typical FFT of Laser Tracker Data

3.4 Off-Nominal Deployment Testing

A variety of off-nominal deployment tests were performed to demonstrate the robustness of the RDA design as predicted by the kinematic model. The first was a "geometry change" test where a .015" spacer was placed under one of the strut mounts and deployment

successfully demonstrated. The second was a "spring energy change" test where full deployment was achieved with a spring removed from the spring damper, forward side strut elbow and aft side strut elbow (3 tests). The third test proved that deployment is insensitive to the order in which the launch restraints were released. The "geometry change" test results also supported validation the kinematic model which is important because the GMI instrument level system performance evaluation uses output from the kinematic model for on-orbit performance predictions. For example a sensitivity coefficient matrix was developed using the kinematic model that predicts the change of reflector orientation due to a linear displacement of any RDA mounting interface. This data is used as part of the instrument level evaluation of beam pointing error due to thermal growth and launch shift.

3.5 Supporting Test Activities

A variety of developmental tests were performed to support manufacturing process development, performance analyses and reliability predictions. For example, multiple configurations of the strut tube / titanium fitting bond joint were evaluated and tested to select the best approach to survive the thermal extremes. Completed strut tube assemblies were subjected to CTE tests to verify values used in stability models. Representative hinge joints underwent life and torque testing in thermal vacuum conditions to demonstrate performance margins. In addition, an EDU bipod compliance mechanism was life tested to demonstrate survival without performance degradation. The EDU was subjected to the worst case predicted number of deflection cycles that the flight assembly will be exposed to during ground testing and launch vibration events. To simplify the test, the predicted deflections throughout the random vibration spectrum were binned into three groups based on 1, 2 and 3 sigma likelihood of occurrence. The EDU mechanism was preloaded to simulate side loads that would be present during vibration and then a motorized test set applied the different deflection cycles in three different tests. Figure 20 shows the test setup.

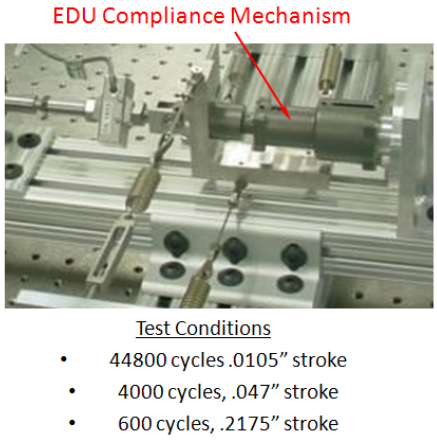

Figure 20: Compliance Mechanism Life Test Setup

3.6 EDU Development / Lessons Learned

The EDU RDA proved to be a valuable tool for the development and functional evaluation of the mechanism. Manufacturing the EDU provided the opportunity to finalize the strut bonding process, work out issues with machining complicated joint features and flesh out assembly and test procedures without the formality associated with the fabrication of flight hardware. Stiffness, repeatability and off-nominal testing of the EDU successfully validated the model predictions and eliminated risk of moving forward with development of the flight assemblies. Deployment testing of the EDU also exposed an unexpected design issue. As the forward side strut elbows straightened at the very end of deployment, the momentum of the hinge caused a spring back phenomenon that would occasionally cause the strut to buckle and not fully deploy. This was remedied prior to flight unit development with the addition of the latch described earlier. Incorporating this latch also provided additional stiffness to the elbow joints adding margin to the deployed stiffness of the RDA structure.

3. CONCLUSIONS

The GMI RDA development and validation program has successfully demonstrated the capability to precisely deploy a payload over a large range of motion in a controlled and reliable manner. The RDA avoids the complexity and reliability concerns associated with a metrology/feedback closed-loop motorized deployment scheme in favor of a passively powered, kinematically determinate approach. The RDA manages this using a lightweight strut design that is inherently flexible until fully deployed where it becomes a rigid structure. This configuration can be tailored for a variety of payload sizes and deployment requirements. The performance demonstrated by the RDA is applicable to the requirements for most RF antennas, as well as a wide range of optical payloads. These other applications would benefit by leveraging the increased understanding and capabilities gained by the RDA program.

4. ACKNOWLEDGEMENTS

Thanks to Greg Compton[2] of ATK for his dedicated effort in the design and development of the RDA and support to the GMI program.
A special thanks to Sergey Krimchansky[3] of GSFC for his technical leadership of GMI and for his support in writing this paper.